Mitochondrial Malic Enzyme 2 Promotes Breast Cancer Metastasis via Stabilizing HIF-1α Under Hypoxia

Duo You
Zhejiang University School of Medicine Second Affiliated Hospital
Danfeng Du
Zhengzhou University First Affiliated Hospital
Xueke Zhao
Zhengzhou University First Affiliated Hospital
Xinmin Li
Women and Infants Hospital of Zhengzhou
Minfeng Ying
Zhejiang University School of Medicine Second Affiliated Hospital
Xun Hu (huxun@zju.edu.cn)
Zhejiang University School of Medicine Second Affiliated Hospital

Research

Keywords: Malate enzyme 2 (ME2), Breast cancer, Metastasis, Malate, α-ketoglutarate (α-KG), Hypoxia-inducible factor-1α (HIF-1α)

Posted Date: January 5th, 2021

DOI: https://doi.org/10.21203/rs.3.rs-138425/v1

Version of Record: A version of this preprint was published at Chinese Journal of Cancer Research on June 1st, 2021. See the published version at https://doi.org/10.21147/j.issn.1000-9604.2021.03.03.

Abstract

Background: α-ketoglutarate (α-KG) is the substrate to hydoxylate collagen and hypoxia-inducible factor-1α (HIF-1α), which are important for cancer metastasis. Previous studies showed that upregulation of collagen prolyl 4-hydroxylase in breast cancer cells stabilizes HIF-1α via depleting α-KG in breast cancer cells. We propose that mitochondrial malate enzyme 2 (ME2) may also affect HIF-1α via modulating α-KG level in breast cancer cells.

Methods: ME2 protein expression was evaluated by immunohistochemistry on 100 breast cancer patients and correlated with clinicopathological indicators. The effect of ME2 knockout on cancer metastasis was evaluated by an orthotopic breast cancer model. The effect of ME2 knockout or knockdown on the levels of α-KG and HIF-1α protein in breast cancer cell lines (4T1 and MDA-MB-231) was determined in vitro and in vivo.

Results: The high expression of ME2 was observed in the human breast cancerous tissues compared to the matched precancerous tissues (P=0.000). The breast cancer patients with a high expression of ME2 had an inferior survival than the patients with low expression of ME2 (P=0.019). ME2 high expression in breast cancer tissues was also related with lymph node metastasis (P=0.016), pathological staging (P=0.033) and vascular cancer embolus (P=0.014). In a 4T1 orthotopic breast cancer model, ME2 knockout significantly inhibited lung metastasis. In the tumors formed by ME2 knockout 4T1 cells, α-KG level significantly increased, collagen hydroxylation level did not change significantly, but HIF-1α protein level significantly decreased, in comparison to control. In cell culture, ME2 knockout or knockdown cells demonstrated a significantly higher α-KG level but significantly lower HIF-1α protein level than control cells under hypoxia. Exogenous malate and α-KG exerted similar effect on HIF-1α in breast cancer cells to ME2 knockout or knockdown. Treatment with malate significantly decreased 4T1 breast cancer lung metastasis. ME2 expression was associated with HIF-1α level in human breast cancer samples (P=0.027).

Conclusion: We provide evidence that upregulation of ME2 is associated with a poor prognosis of breast cancer patients and propose a mechanistic understanding of a link between ME2 and breast cancer metastasis.

Introduction

Worldwide, breast cancer is the most commonly diagnosed cancer and the leading cause of cancer-related death among females (1, 2). The mortality rates of early, locally advanced and metastatic cancers are very different. According to the statistics of American Cancer Society on female breast cancer, the 5-year survival rate is 98% for stage I, 92% for stage II, 75% for stage III, while metastatic disease (stage IV) drops to 27% (3). Metastasis accounts for 90% breast cancer-related death (4, 5). Generation of hypoxia regions and stabilization of hypoxia-inducible factor-1α (HIF-1α) protein are typical features for breast

cancer (6, 7). Accumulated evidence has demonstrated that HIF-1 signaling pathways play important roles in breast cancer metastasis (6, 8).

Previous studies demonstrated that regulation of α-ketoglutarate (α-KG) level could affect the stability of HIF-1α protein in breast cancer cells. It has been demonstrated that collagen prolyl-4-hydroxylase (P4H) expression level is correlated with α-KG level in breast cancer cells (9–11). P4H is upregulated in breast cancer cells (10, 11). The upregulated P4H uses α-KG to hydoxylate collagen thereby reduces cellular α-KG concentration. The reduced α-KG concentration decreases the activity of HIF-1-prolyl hydroxylase (HIF-PHDs) and stabilizes HIF-1α protein, eventually enhancing cancer cell metastasis (9–11).

α-KG is mainly produced in the flux of tricarboxylic acid cycle (TCAC). We propose that mitochondrial malic enzymes (MEs) could potentially regulate α-KG level in breast cancer cells. MEs catalyze the oxidative decarboxylation of malate hence upregulation of MEs could deplete malate in the flux of TCAC and potentially decrease the concentration of TCAC intermediates including α-KG. Mitochondrial MEs include two isoforms, the $NAD(P)^+$-dependent ME2, and the $NADP^+$-dependent ME3 (12–14). As the major isoform in mitochondria of the malic enzymes family (15), knockdown of ME2 by shRNA induces an accumulation of TCAC intermediates in lung cancer cells (16). Up to date, the relationships between ME2 expression and α-KG, between ME2 expression and HIF-1α stability, and between ME2 expression and breast cancer metastasis are unknown.

In this study, we sought to investigate if ME2 knockout or knockdown could decrease HIF-1α protein level via increasing α-KG concentration in breast cancer cells and inhibit breast cancer cell metastasis, for providing a mechanistic understanding of a link between ME2 and breast cancer metastasis.

Materials And Methods

Cells

Breast cancer cell lines 4T1 and MDA-MB-231 were purchased from Cell Bank of Type Culture Collection of the Chinese Academy of Science (Shanghai, China). Cell lines were identified using DNA fingerprinting (SNP for 4T1 and STR for MDA-MB-231) and confirmed to be mycoplasma free. 4T1 was cultured in RPMI-1640 supplemented with 10% FBS and 1% penicillin/streptomycin and 2 mM L-glutamine. MDA-MB-231 was cultured in L15 medium supplemented with 10% FBS and 1% penicillin/streptomycin and 2 mM L-glutamine. A flow cell counter (JIMBIO) was used for cell counting and cell size measurement.

Reagents, enzymes and antibodies

Reagents including the following: ADP (Sigma, A5285); NAD (Sigma, N0632); NADH (Sigma, N8129); malate acid (Sigma, 02288); α-ketoglutaric acid (Sigma, 75890); dimethyl malate (Sigma, 374318); dimethyl 2-oxoglutarate (Sigma, 349631). Enzymes including the following: malic dehydrogenase (Sigma, M2634); L-glutamic dehydrogenase (Sigma, G2501); citrate synthase (Roche, 2168342).

Antibodies including the following: ME2 (Abcam, 139686), HIF-1α (Abcam, 16066), β-actin (HUABIO, M1210-2).

ME2 knockout in 4T1 cells

The ME2 was knocked out using Crispr-Cas9 system in 4T1 cells following a standard protocol (17). The designed sgRNA sequences were as follows:

ME2 forward: CACCGTTACAAGAGCGACAAATGCT,

ME2 reverse: AAACAGCATTTGTCGCTCTTGTAAC.

A pSpCas9 (BB)-2A-Puro (PX459) V2.0 plasmid (Addgene, #62988) was used as sgRNA expression vector and Lipofectamine 3000 (Invitrogen) was used to transfected the constructed plasmids into cells. Cells were selected by puromycin and assessed the cleavage efficiency by T7 Endonuclease I. Cultured the monoclonal cell lines and detected the microdeletion by PCR and Sanger sequencing. Check the candidate off-target sites by sequencing to avoid off-target effect. The effect of ME2 knockout was checked by Western blot using anti-ME2 antibodies (Supplementary Figure. S1B).

ME2 knockdown in MDA-MB-231 cells

For ME2 knockdown in MDA-MB-231 cells, three specific shRNA were chemically synthesized by Sangon Biotech (Shanghai, China). The three ME2 shRNA sequence used in this study were as follows:

ishME2#1: (CCGGCGGCATATTAGTGACAGTGTTCTGCAGAACACTGTCACTAATATGCCGTTTTTG)

ishME2#2:

(CCGGCCCAGTATGGACACATCTTTACTGCAGTAAAGATGTGTCCATACTGGGTTTTTG)

ishME2#3: (CCGGGCACGGCTGAAGAAGCATATACTGCAGTATATGCTTCTTCAGCCGTGCTTTTTG)

Expression plasmids for ME2 shRNA were made in pLKO.1-puro vector (Addgene, #10879) using a protocol provided by Addgene. The shME2-expressing pLKO.1 vector was introduced into cancer cell lines by lentiviral infection. Recombinant lentiviral particles were produced by transient transfection of 293T cells following a standard protocol. Briefly, cells were maintained in standard culture conditions without any antibiotic. Cotransfected the recombinant pLKO.1-shME2 plasmid into HEK293T cells with the packaging vectors. Viral supernatant was harvested 72 hours after transfection, centrifuged to remove any 293T cells and purified by ultracentrifugation. For transduction, the packaged pLKO.1-shME2 lentiviral particles were added to cell culture medium containing 4 μg/mL polybrene. After infection 72 hours, cells were selected using 1.5 μg/ml puromycin and the effect of knockdown was checked by Western blot using anti-ME2 (Abcam) antibodies (Supplementary Figure. S1C). A non-targeting shRNA (shPLKO) was used as a control.

Hypoxia treatment of cells

Cells were seeded into 10 cm dishes and incubate in normoxia incubator overnight. Then replace the medium with standard medium (supplemented with 10% FBS and 2 mM L-glutamine without any antibiotic) when the culture reached 70-80% confluences the next day. For exogenous α-KG treatment, replace the medium with standard medium supplemented with 0.5mM or 1mM dimethyl α-KG. For exogenous malate treatment, replace the medium with standard medium supplemented with 10mM or 20mM dimethyl malate. Then cells were tansfered into a hypoxic culture chamber (ELECTROTEK, England) and incubated for 4 hours with 1% oxygen and carbon 5% dioxide concentration.

Western blot

Cells and tumor tissues were lysed with M-PERTM mammalian protein extraction reagent (Thermo Fisher Scientific). Protein concentration was determined using BCA protein assay kit (Thermo Fisher Scientific). Briefly, 1.5×10^6 4T1 or 8×10^5 MDA-MB-231 cells were seeded in a 6-well plate, after hypoxia treatment of cells, rinsed with ice-cold PBS twice, add 80 μl ice-cold M-PERTM containing protease inhibitor (Master of Small Molecules), scraped the plates and removed the cell suspension into eppendorf tube. All the above operations were carried out in the hypoxia incubator with oxygen concentration in 1%. Then centrifuge the cell suspension at 15,000 g for 5 minutes at 4°C. The supernatant was collected and boiled for 10 min mixed with loading buffer containing 100 mM DTT, and 40 μl protein extract were separated by 10% SDS-PAGE, transferred to PVDF membranes, and 5% bovine serum albumin blocked for 1 hour, and then incubated with primary antibodies (β-actin 1:5000; ME2 1:2000; HIF-1α 1:1000) overnight at 4℃. The HRP conjugated secondary antibodies (1:5000) were added and bands were visualized by enhanced chemiluminescence (Tanon, China).

For tumor tissue protein extraction, 50 mg tumor tissue was minced, mixed with 1.5ml ice-cold M-PERTM containing protease inhibitor, and then homogenized. The homogenized tissue was centrifuged at 15,000 g for 10 minutes at 4°C. The supernatant was collected and 40 μl sample was mixed with loading buffer for Western blot as described above.

Enzymatic determination of malate, α-ketoglutarate and citrate

After hypoxia treatment, cells were harvested by the following describe: rinsed with ice-cold PBS thrice, add 1.2 ml 80% (vol/vol) methanol per well, then scrape the plates and remove the cell suspension into eppendorf tube. All the above operations were carried out in the hypoxia incubator with oxygen concentration in 1%. Vortex the lysate/methanol mixture and centrifuge at 25,000 g for 10 min at 4℃ to remove the debris. Evaporated the supernatant completely, dissolved the lyophilized sample in 400 μl double distilled water, centrifuge at 25,000 g for 10 min at 4℃ and collected supernatant for subsequent metabolite determination. For tumor tissue, 200 mg tumor tissue was minced and added 1ml ice-cold 80% (vol/vol), and then fully crushed by homogenizer on ice. Vortex the mixture and centrifuge at 25,000 g for 10 min at 4℃. Evaporated the supernatant, dissolved the lyophilized sample in 400 μl double distilled water, centrifuge and collect supernatant as described above. The concentrations of metabolite

were measured using a spectrophotometer (Beckman Coulter) according to the methods described previously with some modifications (18).

Assay of malate: Add 20 µl sample to 980 µl reaction buffer (200 mM Glycine, 170 mM hydrazine, 2 mM NAD^+, 2.1U/ml malic dehydrogenase, pH 9.2). Mix well and incubate at room temperature for 1 hour, and read at 340 nm against the blank. Add 20 µl sample to the cuvette which contains the same ingredients but the enzyme simultaneously to correct the drift effect.

Assay of α-ketoglutarate: Add 100 µl sample to 900 µl reaction buffer (40 mM imidazole, 20 mM acetate, 25 mM ammonim acetate, 100 µM ADP, 100 µM NADH, 0.15 U/ml L-glutamic dehydrogenase). Mix well and incubate at room temperature for 15 min, and read at 340 nm against the blank. Add 100 µl sample to the cuvette which contains the same ingredients but the enzyme simultaneously to correct the drift effect.

Assay of citrate: Add 50 µl sample to 950 µl reaction buffer (25 mM Tris-base, 75 mM Tris in the hydrochloride, 100 µM NADH, 40 µM $ZnCL_2$, 0.12 U/ml citrate lyase, 0.3U/ml malic dehydrogenase, pH 7.6). Mix well and incubate at room temperature for 10 min, and read at 340 nm against the blank. Add 50 µl sample to the cuvette which contains the same ingredients but the enzyme simultaneously to correct the drift effect.

Transfection of 4T1 cell with luciferase gene

The recombinant-retrovirus containing the expressing luciferase gene vector was production by Genechem. According to the manufacturer's instructions, $4T1_{PX459}$ or $4T1_{ME2KO}$ cells were seeded in a 6-well plate and the retrovirus were added to cell culture medium containing 4 µg/mL polybrene. After infection 72 hours, cells were selected using G418. The surviving cells were designated as $4T1_{PX459\text{-}Luciferase}$ or $4T1_{ME2KO\text{-}Luciferase}$. The in vitro luciferase activity of the cells was conducted by using a standard approach. A total of 8×10^5 of cells were collected and lysed in 1X passive lysis buffer (PLB). 98 µl cell lysate, 2 µl luciferin stock solution (15mg/ml) and 100 µl luciferase assay buffer (200mM Tris- HCl pH 7.8, 10mM $MgCl_2$, 5000 µM CoA, 300 µM ATP) were mixed, and the absorbance at 560 nm was read.

Orthotopic tumor growth and metastasis assays in mouse model

Six-week-old female BALB/c mice were randomly assigned into two groups (n=6 per group) and orthotopically inoculated with 1×10^5 $4T1_{PX459}$ or $4T1_{ME2KO}$ cells near the second right mammary fat pad. Mouse weight and tumor size was measured once a week, and tumor volume (V) was calculated by the formula: tumor volume [cm^3] = [length (cm) × width (cm) ^{2} × 0.5]. Sacrificed the mouse after 5 weeks, record tumor weight and scored the lung metastasis by counting the macroscopic metastatic nodules. In order to present the lung metastasis intuitively, $4T1_{PX459\text{-}Luciferase}$ or $4T1_{ME2KO\text{-}Luciferase}$ cells were orthotopically inoculated as described above. Live animal bioluminescence imaging was used to image the tumor and lung every weeks after implantation (Caliper IVIS system, PerkinElmer). Isoflurane-

anesthetized mice were injected intraperitoneally with D-luciferin substrate (YEASEN; 15 mg/ml in phosphate buffer saline) and were imaged after 10 minutes. All animal experiments were complied with the ARRIVE guidelines and the National Institutes of Health guide for the care and use of Laboratory animals, and were approved by the Committee of Animal Experimental Centre at the Zhejiang Chinese Medical University.

Malate treatment in mouse model

1×10^5 4T1 cells were implanted orthotopically into mammary fat pads of BALB/c mice (n=12). Mice were randomly divided into two groups (n=6/per group). Malate treatment group was injected intraperitoneally with malate (50mg/kg, dissolved in phosphate buffer saline) once a day for three weeks. Control group was injected intraperitoneally with equal volume of phosphate buffer saline as control.

Hydroxyproline detection in mouse tumor tissue

Hydroxyproline is found almost exclusively in the protein collagen the hydroxyproline has been used as a marker to quantify levels of tissue collagen. The total amount of hydroxyproline was measured by the Hydroxyproline Assay Kit (Nanjing Jiancheng Bioengineering Institute) according to the manufacturer's protocol.

Patients

One hundred female breast cancer patients were retrospectively retrieved in this study from a database, which has been established by The State Key Laboratory of Esophageal Cancer Prevention & Treatment and Henan Key Laboratory of Esophageal Cancer Research in The First Affiliated Hospital of Zhengzhou University. All the patients had been underwent mastectomy from August 2012 to December 2014 without any radiation therapy or chemotherapy prior to surgery before operation. All the patients had the detailed clinicohistopathological record. Staging for breast cancer were based on American Joint Committee on Cancer (AJCC) TNM staging system in 2017 (19). All of them were females with a mean age was 48.39 ± 11.13 years, with a median age of 46 years (range from 26 to 82 years). The last follow-up was March 2020. Overall survival (OS) time was calculated from the day of mastectomy to death or to the last follow-up date. The median follow-up of the entire cohort was 70.5 months (range 11.7–91.0 months). Informed consent was obtained from patients in this study. The study protocol was in accordance with The Code of Ethics of the World Medical Association (Declaration of Helsinki) for experiments involving humans and approved by the Medical Ethics Committee of Zhengzhou University.

Immunohistochemical analysis

A total of 100 breast cancer tissues and 82 matched adjacent non-cancerous tissues were collected from surgically resected specimens. Histopathological diagnoses were based on WHO criteria in 2012 (20). The tissues were routinely 10% neutral formalin fixed, paraffin-embedded and then sectioned. Serial 4 μm sections were prepared for histopathological analysis (hematoxylin and eosin stain) and

immunohistochemical staining. Follow the manufacturer's instructions, tissue sections were deparaffinized, rehydrated, subjected to antigen retrieval. The samples were incubated with primary antibody (ME2: 1:75, HIF-1α: 1:200) overnight at 4 °C. The secondary antibody was conjugated to horseradish peroxidase. The immunoreactivty was visualized through adding diaminobenzidine and subsequently counterstained with hematoxylin. The sections were evaluated under microscope by two pathologists independently who were blinded to the patients' clinical information.

According to immunohistochemical scoring system described previously (21, 22), ME2 immunostaining score (S) was determined semiquantitatively by multiplying the percentage of positive cells (P) with intensity (I), according to the formula: S= P×I. The range score for percentage of positive cells is 0 to 4 (0, 0–10%; 1, 11%-25% scores; 2, 26%-50%; 3, 51%-75%; 4, 76%-100%). The range score for intensity is 0 to 3 (0, no staining; 1, weak; 2, moderate; 3, strong.). The index score was obtained a range from 0 to 12. The final immunostaining results were denoted as low expression of ME2 (≤6 scores) and high expression of ME2 (>6 scores). As active HIF-1α is commonly assumed to be located in the nucleus, nuclear staining was evaluated as being positive (23, 24), cytoplasmic staining was observed in some cases but was not recorded. The positive staining for HIF-1α was defined as nuclear staining in ≥10% of the tumor cells.

Statistical analysis

Statistical analyses were conducted using IBM SPSS version 21.0. Quantitative data were represented as the mean ± standard and the Student's t test was applied. Categorical data were represented as frequency (number-percent). Relationships of ME2 expression and clinicopathological features were evaluated by the chi-square (χ^2-value). The Kaplan–Meier survival analysis was used to estimate the association between eligible variables and survival. Cox proportional hazards regression models were used for multivariate survival analysis in stepwise regression manner. Any result with a P-value of less than 0.05 was considered as statistically significant.

Results

ME2 is associated with a poor prognosis in breast cancer patients

If ME2 is associated with breast cancer metastasis, ME2 expression of breast cancer should be inversely correlated with the survival of breast cancer patient. This is the first question we want to address.

We retrieved 100 breast cancer patients. Table 1 summarized the clinicopathological characteristics of the patients. All the patients were confirmed as breast cancer, and were predominately at the invasive stage (92%), only 8% at CIS stage. Of the patients in this study, more than half of the patients were in T2 (63%), followed by T1 (26%), Tis (8%) and T3 (3%). And almost half of the patients (42%) had positive lymph node metastasis when they were diagnosed. 72% of the patients were in earlier stage based on

pathological staging, including 8% patients in stage 0, 20% in stage I and 44% in stage II and the rest (28%) patients were in advanced stage III (Table 1).

Table 1
Clinicopathological characteristics of 100 breast cancer patients

Variables	No. of patients examined N (%)
Age	
< 50 years	60 (60.0)
≥ 50 years	40 (40.0)
Gender	
Male	0 (0)
Female	100 (100.0)
Urban and rural regions	
rural	64 (64.0)
urban	36 (36.0)
T staging	
Tis	8 (8.0)
T1	26 (26.0)
T2	63 (63.0)
T3	3 (3.0)
Lymph node metastasis	
Yes	42 (42.0)
No	58 (58.0)
Pathological staging	
0	8 (8.0)
I	20 (20.0)
II	44 (44.0)
III	28 (28.0)

The immunohistochemical (IHC) staining analyses were performed on the 100 breast cancer specimens, which showed that the immunoreactivity for ME2 protein was located in the cytoplasm both in breast cancerous and precancerous tissues (Figure. 1A). High expression of ME2 was displayed in breast cancerous tissues (63.0%, 63/100) compared to the matched precancerous tissues (34.1%, 28/82) ($\chi2$ = 18.803, P = 0.000, Figure. 1B).

The breast cancer patients with high expression of ME2 had an inferior survival than the patients with low expression of ME2 ($\chi2$ = 5.527, P = 0.019, Figure. 1C).

Me2 Is Associated With Metastasis-related Indicators

The association of ME2 expression with clinicopathological indicators was also assessed in this study. ME2 high expression was associated with lymph node metastasis ($\chi2$ = 5.405, P = 0.016), pathological staging ($\chi2$ = 4.118, P = 0.033), and vascular cancer embolus ($\chi2$ = 5.596, P = 0.014), which were the clinicopathological indicators that significantly correlated with metastasis and progression in breast cancer (Table 2).

Table 2
Relationship between ME2 expression and clinicopathological indicators in breast cancer

Variables	No. of patients examined	Expression of ME2 protein		χ2	P
		High (N = 63) N (%)	Low (N = 37) N (%)		
Age				1.401	0.166
< 50 years	60	35 (58.3)	25 (41.7)		
≥ 50 years	40	28 (70.0)	12 (30.0)		
T staging					
Tis + T1	34	19 (55.9)	15 (44.1)	1.120	0.200
T2 + T3	66	44 (66.7)	22 (33.3)		
Lymph node metastasis				5.405	**0.016**
No	58	31 (53.4)	27 (46.6)		
Yes	42	32 (76.2)	10 (23.8)		
Pathological staging				4.118	**0.033**
0 + I + IIA	60	33 (55.0)	27 (45.0)		
IIB + III	40	30 (75.0)	10 (25.0)		
Vascular cancer embolus				5.596	**0.014**
No	83	48 (57.8)	35 (42.2)		
Yes	17	15 (88.2)	2 (11.8)		
ER status				0.018	0.53
Negative	37	23 (62.2)	14 (37.8)		
Positive	63	40 (63.5)	23 (36.5)		
PR status				2.581	0.081
Negative	40	29 (72.5)	11 (27.5)		
Positive	60	34 (56.7)	26 (43.3)		
Her-2 status				0.429	0.807
Negative	42	25 (59.5)	17 (40.5)		
Positive	36	24 (66.7)	12 (33.3)		

Variables	No. of patients examined	Expression of ME2 protein		χ2	P
		High (N = 63) N (%)	Low (N = 37) N (%)		
Not available	22	14 (63.6)	8 (36.4)		
Ki67 index				0.249	0.395
≤14%	24	14 (58.3)	10 (41.7)		
14%	75	48 (64.0)	27 (36.0)		

Furthermore, in this study, lymph node metastasis put a clear association for poor prognosis (χ2 = 10.989, P = 0.001, Figure. 2A). Pathological staging was divided into earlier staging (0-IIA) and advanced staging (IIB-III). The advanced staging was worse indicator for survival compare to the earlier staging (χ2 = 12.711, P = 0.000, Figure. 2D). In the subgroup analysis, high expression of ME2 exhibited more significant worse prognostic impact in the subgroup of patients with no lymph node metastasis (χ2 = 4.664, P = 0.031, Figure. 2B), earlier pathological staging (0-IIA) (χ2 = 4.362, P = 0.037, Figure. 2E) or without vascular cancer embolus (χ2 = 6.473, P = 0.011, Figure. 2H). Whereas, in the subgroup of patients with lymph node metastasis (χ2 = 0.374, P = 0.541, Figure. 2C), advanced staging (χ2 = 0.565, P = 0.452, Figure. 2F) or with positive vascular cancer embolus (χ2 = 0.184, P = 0.668, Figure. 2I), ME2 expression has no difference in survival.

No significant association was observed between ME2 expression and age group, or T staging, ER status, PR status, Her-2 status, Ki67 index (Table 2). Age group, T staging and vascular cancer embolus were no statistical survival difference in this study (Supplementary Table S1). The multivariate cox regression analysis demonstrated that only lymph node metastasis was the independent prognostic factor for breast cancer patient survival (χ2 = 3.878, P = 0.010, Supplementary Table S1).

Me2 Knockout Significantly Inhibits Lung Metastasis

The above results demonstrated that ME2 expression was closely associated with breast cancer patient survival and with metastasis-related indicators. The next question is to validate the relationship between ME2 and breast cancer metastasis. We manipulated ME2 knockout in 4T1 cell ($4T1_{ME2KO}$) (Supplementary Figure. S1.) and We inoculated $4T1_{ME2KO}$ and control cell $4T1_{PX459}$ into the mammary pad of BALB/c mice. The 2 groups of mice showed similar body weights and tumor growths (Figure. 3A-C). However, knockout of ME2 nearly abolished 4T1 lung metastasis (Figure. 3D-F). These results provided evidence that ME2 enhances breast cancer metastasis.

ME2 knockout increases α-KG concentration and decreases HIF-1α protein level in breast cancer cells in vivo

Next, we determined if ME2 knockout increases α-KG concentration and decreases HIF-1α levels in tumors. α-KG level, together with malate and citrate, was increased in in $4T1_{ME2KO}$-derived tumor in comparison to control tumors (Figure. 4A-C). As the substrate of 2-oxoglutarate dependent oxygenases, α-KG is known to be involved in collagen stabilization and HIF-1α degradation (25, 26), both of which are correlated with tumor metastasis. Then we detected level of collagen hydroxyproline and HIF-1α in tumors formed by ME2 knockout 4T1 and control cells. While the level of collagen hydoxyproline was comparable between 2 groups (Figure. 4D), HIF-1α protein level was significantly higher in ME2 knockout group than in control group (Figure. 4E-G).

ME2 knockout or knockdown increases α-KG concentration and decreases HIF-1α level in breast cancer cells under hypoxia

The above results suggested that ME2 knockout increased α-KG level and decreased HIF-1α protein level but it does not necessarily indicate that the increased α-KG and decreased HIF-1α level is directly linked to ME2, because cancer cells in vivo are in a complex and dynamic environment. To further link the relationship between ME2, α-KG, and HIF-1α, we measured the α-KG level and HIF-1α protein levels in ME2 knockout cell $4T1_{ME2KO}$ and ME2 knockdown cell MDA-MB-231_{shME2} cultured under hypoxia. The characterization of cells was shown in Supplementary Figure. S1.

HIF-1α protein level in the ME2 knockout or knockdown cell was significantly lower than that in control cells (Figure. 5A & B), while cellular α-KG concentration were significantly higher in the in ME2 knockout or knockdown cell (Figure. 5C & D). Besides α-KG, malate and citrate concentrations also increased in ME2 knockout or knockdown cells (Figure. 5C & D).

To link α-KG with HIF-1α under hypoxia, we added dimethyl α-KG into cell culture. Dimethyl α-KG is a cell membrane permeable ester, once it crosses the cell membrane, it is hydrolyzed by esterase to generate α-KG. We observed that dimethyl α-KG significantly reduced HIF-1α concentrations in 4T1 or MDA-MB-231 cells (Figure. 5E & F).

The direct consequence of ME2 knockout or knockdown is the accumulation of malate, hence adding exogenous malate may mimic the effect of ME2 inhibition. Indeed, exogenous dimethyl malate significantly increased the concentrations of α-KG, malate, and citrate (Figure. 6A & B) and reduced HIF-1α protein level in 4T1 or MDA-MB-231 cells under hypoxia (Figure. 6C & D).

Malate treatment significantly inhibits lung metastasis of 4T1 breast cancer cells

Since ME2 knockout significantly suppresses 4T1 lung metastasis, we ask if malate treatment could also inhibit breast cancer metastasis. 4T1 cells were implanted orthotopically into mammary fat pads of BALB/c mice. Mice were randomly divided into two groups and injected intraperitoneally with phosphate buffer saline (control) or malate (50 mg/kg, dissolved in PBS) once a day for three weeks. While there was no significant difference in the mouse body weight and tumor volume between 2 groups (Figure. 6E & F), the metastatic nodules in lung in the malate treatment group significantly reduced (Figure. 6G & H).

ME2 is associated with HIF-1α expression in human breast cancer

To correlate ME2 with HIF-1α in clinical breast cancer, we examined the expression of HIF-1α and ME2 in breast cancer tissues. The immunoreactivities of HIF-1α were located mostly in the nuclei and the cytoplasmic staining was observed in some cases. Of the clinical breast cancer patients, we randomly selected 20 patients with low expression of ME2 and 20 patients with high expression of ME2, the positive HIF-1α expression rates were 30.0% (6/20) in ME2-expression low patients and 65.0% (13/20) in ME2-expression high patients, respectively ($\chi 2 = 4.912$, $P = 0.027$, Figure. 7B). The data showed that ME2 expression was significantly correlated with HIF-1α expression in human breast cancer.

Discussion

Breast cancer metastasis is closely associated with hypoxia (7, 27). The partial pressure of O_2 in breast cancer with median value is 10 mm Hg, in contrast to 65 mm Hg in normal human breast tissue (28, 29). Hypoxia enhances hypoxia-inducible factor-1 signaling, which increased the risk of metastasis (8, 30, 31). HIF-1 targeted genes included cell survival, angiogenesis, metabolism, immortalization, metastasis, resistance to therapy (6, 32, 33). Therefore, stabilization of HIF-1 is crucial for breast cancer progression. HIF-1 is composed of 2 subunits, HIF-1α and HIF-1β. HIF-1β is constitutively expressed and is stable whereas HIF-1α is sensitive to oxygen level. In the presence of oxygen, α-KG, and Fe^{2+}, HIF-PHDs hydroxylate HIF-1α and target it for proteasome degradation. The activity of HIF-1 is determined by the stability of HIF-1α, while the stability of HIF-1α is determined largely by the activity of HIF- PHDs (34–36). Other factors could also influence the stability of HIF-1α. To hydroxlyate HIF-1α, HIF1-PHDs also require α-KG as substrate, so that a dioxygen is incorporated into 2 substrates, HIF-1α and α-KG.

Enzymologically, the concentrations of oxygen and α-KG both affect the activity HIF-PHDs. When oxygen level is low, increasing α-KG could enhance the activity of HIF1-PHD and decreasing the stability of HIF-1α in breast cancer cells. Previous studies also demonstrated that modest variations of α-KG concentrations could significantly change HIF-PHDs activity (26, 37, 38). Moreover, α-KG is not only the substrate but also an allosteric activator of HIF1-PHDs by increasing its affinity for oxygen, thereby destabilizing HIF-1α at very low concentrations of oxygen (39, 40). Previously, Dr. Xu's group identified a pathway to regulate α-KG levels by P4H in breast cancer cells: the high expression of P4H in breast cancer cells use α-KG to hydroxylate collagen hence deplete α-KG level in breast cancer cell, thereby stabilizing HIF-1α protein and promoting breast cancer metastasis (9–11).

α-KG was mainly produced from the flux of TCAC. In the flux of TCAC, malate could be dehydrogenated by malate dehydrogenase to produce NADH and oxaloacetate, or catalyzed by ME2 to generate NAD(P)H and pyruvate through oxidative decarboxylation. ME2 compete with malate dehydrogenase for malate, therefore reducing the flux from malate to oxaloacetate and to TCAC. Down-regulating ME2 caused a large accumulation of malate in breast cancer cells. Under hypoxia, as oxidative phosphorylation would be inhibited (41–43) and NADH/NAD ratio would increase (44, 45), we assume that the intermediates in the TCAC flux would be thermodynamically re-equilibrated. This re-equilibration would lead to an increase

of other TCAC intermediate levels including α-KG. We showed that ME2 knockout or knockdown increased not only malate, but also α-KG and citrate level in breast cancer cells exposed to hypoxia. The increased level of α-KG was associated with a decreased level of HIF-1α protein. Exogenous malate and α-KG exerted a similar effect on HIF-1α as ME2 knockdown or knockout. All these lines of evidence suggested that ME2 knockdown or knockout reduces HIF-1α protein level via increasing α-KG level in breast cancer cells. As it is well documented that HIF-1 signaling pathways play important roles in breast cancer metastasis (32, 33, 46), we propose that metastasis inhibition induced by ME2 knockout or knockdown could be interpreted by the following steps, ME2 knockout induces accumulation of TCAC intermediates including α-KG, which enhances HIF1-PHD activity, which destabilizes HIF-1α, eventually inhibiting HIF-1α-mediated metastasis signaling.

The clinical evidence also suggests that ME2 expression is associated with breast cancer metastasis. The patients with high expression of ME2 had a worse survival than those with low expression of ME2. ME2 high expression was related to lymph node metastasis, positive vascular cancer embolus and pathological staging progression, all of which are key indicators leading to poor prognosis in breast cancer patients. As metastasis accounts for 90% breast cancer related death (4, 5), and as high expression of ME2 is significantly correlated with death rate (Figure. 1C), we speculate a close link between ME2 expression and breast cancer metastasis. Using 4T1 orthotopic breast cancer in vivo model, we provided evidence that ME2 knockout nearly completely inhibited 4T1 cell lung metastasis.

Conclusion

In conclusion, we provide experimental and clinical evidence that ME2 plays a part in breast cancer metastasis and interpret an underlying mechanism by which ME2 promotes breast cancer metastasis.

Abbreviations

HIF-1α: Hypoxia-inducible factor 1α; α-KG: α-ketoglutarate; P4H: Prolyl-4-hydroxylase; HIF-PHDs: HIF1-prolyl hydroxylases; TCAC: Tricarboxylic acid cycle; MEs: Malic enzymes; ME2: Malic enzyme 2; IHC: immunohistochemical; OS: Overall survival.

Declarations

Ethics approval and consent to participate

All animal experiments were complied with the ARRIVE guidelines and the National Institutes of Health guide for the care and use of Laboratory animals, and were approved by the Committee of Animal Experimental Centre at the Zhejiang Chinese Medical University. Extensive efforts were made to ensure minimal usage of animals as well as their suffering. The human study protocol was in accordance with The Code of Ethics of the World Medical Association (Declaration of Helsinki) for experiments involving

humans were approved by the Medical Ethics Committee of Zhengzhou University. Informed consent was obtained from patients in this study.

Consent for publication

All authors agree to submit the article for publication.

Availability of data and materials

The datasets used and/or analyzed during the current study are available from the corresponding author on reasonable request.

Competing interests

The authors declare that they have no competing interests.

Funding

This work has been supported in part by the China National 973 project (2013CB911303), China Natural Sciences Foundation projects (81470126), a key project (2018C03009) funded by Zhejiang Provincial Department of Sciences and Technologies, and the Fundamental Research Funds for the Central Universities, National Ministry of Education, China, to XH.

Authors' contributions

Duo You: Methodology, Formal analysis, Data curation, Writing - Original Draft; Danfeng Du and Xinmin Li: Methodology, Investigation; Xueke Zhao and Minfeng Ying: Investigation, Resources; Hu Xun: Conceptualization, Supervision, Writing - Review & Editing. All authors read and approved the final manuscript.

Acknowledgments

The authors would like to thank Zongmin Fan for excellent technical support.

Author details

[1]Cancer Institute, The Second Affiliated Hospital, Zhejiang University School of Medicine, Hangzhou 310000, China. [2]The State Key Laboratory of Esophageal Cancer Prevention & Treatment and Henan Key Laboratory of Esophageal Cancer Research of The First Affiliated Hospital, Zhengzhou University, Zhengzhou 450000, China. [3]Department of Pathology, Women and Infants Hospital of Zhengzhou, Zhengzhou 450000, China.

References

1. Bray F, Ferlay J, Soerjomataram I, Siegel RL, Torre LA, Jemal A. Global cancer statistics 2018: GLOBOCAN estimates of incidence and mortality worldwide for 36 cancers in 185 countries. CA Cancer J Clin. 2018;68(6):394–424.
2. Miller KD, Nogueira L, Mariotto AB, Rowland JH, Yabroff KR, Alfano CM, et al. Cancer treatment and survivorship statistics, 2019. CA Cancer J Clin. 2019;69(5):363–85.
3. DeSantis CE, Ma J, Gaudet MM, Newman LA, Miller KD, Goding Sauer A, et al. Breast cancer statistics, 2019. CA Cancer J Clin. 2019;69(6):438–51.
4. Gupta GP, Massague J. Cancer metastasis: building a framework. Cell. 2006;127(4):679–95.
5. Lambert AW, Pattabiraman DR, Weinberg RA. Emerging Biological Principles of Metastasis Cell. 2017;168(4):670–91.
6. Gilkes DM, Semenza GL. Role of hypoxia-inducible factors in breast cancer metastasis. Future Oncol. 2013;9(11):1623–36.
7. Semenza GL. Defining the role of hypoxia-inducible factor 1 in cancer biology and therapeutics. Oncogene. 2010;29(5):625–34.
8. Wong CC, Gilkes DM, Zhang H, Chen J, Wei H, Chaturvedi P, et al. Hypoxia-inducible factor 1 is a master regulator of breast cancer metastatic niche formation. Proc Natl Acad Sci U S A. 2011;108(39):16369–74.
9. Xiong G, Stewart RL, Chen J, Gao T, Scott TL, Samayoa LM, et al. Collagen prolyl 4-hydroxylase 1 is essential for HIF-1alpha stabilization and TNBC chemoresistance. Nat Commun. 2018;9(1):4456.
10. Gilkes DM, Chaturvedi P, Bajpai S, Wong CC, Wei H, Pitcairn S, et al. Collagen prolyl hydroxylases are essential for breast cancer metastasis. Cancer Res. 2013;73(11):3285–96.
11. Xiong G, Deng L, Zhu J, Rychahou PG, Xu R. Prolyl-4-hydroxylase α subunit 2 promotes breast cancer progression and metastasis by regulating collagen deposition. BMC Cancer. 2014;14(1):1–12.
12. Chang G-G, Tong L. Structure and function of malic enzymes, a new class of oxidative decarboxylases. Biochemistry. 2003;42(44):12721–33.
13. Loeber G, Infante A, Maurer-Fogy I, Krystek E, Dworkin M. Human NAD (+)-dependent mitochondrial malic enzyme. cDNA cloning, primary structure, and expression in Escherichia coli. J Biol Chem. 1991;266(5):3016–21.
14. Loeber G, Maurer-Fogy I, Schwendenwein R, Purification. cDNA cloning and heterologous expression of the human mitochondrial NADP+-dependent malic enzyme. Biochem J. 1994;304(3):687–92.
15. Jiang P, Du W, Mancuso A, Wellen KE, Yang X. Reciprocal regulation of p53 and malic enzymes modulates metabolism and senescence. Nature. 2013;493(7434):689–93.
16. Ren JG, Seth P, Clish CB, Lorkiewicz PK, Higashi RM, Lane AN, et al. Knockdown of malic enzyme 2 suppresses lung tumor growth, induces differentiation and impacts PI3K/AKT signaling. Sci Rep. 2014;4:5414.
17. Ran FA, Hsu PD, Wright J, Agarwala V, Scott DA, Zhang F. Genome engineering using the CRISPR-Cas9 system. Nat Protoc. 2013;8(11):2281–308.

18. Passonneau JV, Lowry OH. Enzymatic analysis: a practical guide: Springer Science & Business Media; 1993.
19. Amin MB, Greene FL, Edge SB, Compton CC, Gershenwald JE, Brookland RK, et al. The Eighth Edition AJCC Cancer Staging Manual: Continuing to build a bridge from a population-based to a more "personalized" approach to cancer staging. CA Cancer J Clin. 2017;67(2):93–9.
20. Frank GA, Danilova NV, Andreeva I, Nefedova NA. [WHO classification of tumors of the breast, 2012]. Arkh Patol. 2013;75(2):53–63.
21. Fitzgibbons PL, Dillon DA, Alsabeh R, Berman MA, Hayes DF, Hicks DG, et al. Template for reporting results of biomarker testing of specimens from patients with carcinoma of the breast. Arch Pathol Lab Med. 2014;138(5):595–601.
22. Fedchenko N, Reifenrath J. Different approaches for interpretation and reporting of immunohistochemistry analysis results in the bone tissue - a review. Diagn Pathol. 2014;9:221.
23. Potharaju M, Mathavan A, Mangaleswaran B, Patil S, John R, Ghosh S, et al. Clinicopathological Analysis of HIF-1alpha and TERT on Survival Outcome in Glioblastoma Patients: A Prospective, Single Institution Study. J Cancer. 2019;10(11):2397–406.
24. Nalwoga H, Ahmed L, Arnes JB, Wabinga H, Akslen LA. Strong Expression of Hypoxia-Inducible Factor-1alpha (HIF-1alpha) Is Associated with Axl Expression and Features of Aggressive Tumors in African Breast Cancer. PLoS One. 2016;11(1):e0146823.
25. Ge J, Cui H, Xie N, Banerjee S, Guo S, Dubey S, et al. Glutaminolysis promotes collagen translation and stability via α-ketoglutarate–mediated mTOR activation and proline hydroxylation. Am J Respir Cell Mol Biol. 2018;58(3):378–90.
26. Tennant DA, Frezza C, MacKenzie ED, Nguyen QD, Zheng L, Selak MA, et al. Reactivating HIF prolyl hydroxylases under hypoxia results in metabolic catastrophe and cell death. Oncogene. 2009;28(45):4009–21.
27. Rankin EB, Giaccia AJ. Hypoxic control of metastasis. Science. 2016;352(6282):175–80.
28. Vaupel P, Hockel M, Mayer A. Detection and characterization of tumor hypoxia using pO2 histography. Antioxid Redox Signal. 2007;9(8):1221–35.
29. Vaupel P, Mayer A, Briest S, Höckel M. Oxygenation gain factor: a novel parameter characterizing the association between hemoglobin level and the oxygenation status of breast cancers. Cancer research. 2003;63(22):7634–7.
30. Lu X, Kang Y. Hypoxia and hypoxia-inducible factors: master regulators of metastasis. Clin Cancer Res. 2010;16(24):5928–35.
31. Rankin EB, Nam JM, Giaccia AJ. Hypoxia: Signaling the Metastatic Cascade. Trends Cancer. 2016;2(6):295–304.
32. Semenza GL. Targeting HIF-1 for cancer therapy. Nat Rev Cancer. 2003;3(10):721–32.
33. Unruh A, Ressel A, Mohamed HG, Johnson RS, Nadrowitz R, Richter E, et al. The hypoxia-inducible factor-1 alpha is a negative factor for tumor therapy. Oncogene. 2003;22(21):3213–20.

34. Fong GH, Takeda K. Role and regulation of prolyl hydroxylase domain proteins. Cell Death Differ. 2008;15(4):635–41.
35. Berra E, Benizri E, Ginouvès A, Volmat V, Roux D, Pouysségur J. HIF prolyl-hydroxylase 2 is the key oxygen sensor setting low steady-state levels of HIF-1α in normoxia. EMBO J. 2003;22(16):4082–90.
36. Lee J-W, Bae S-H, Jeong J-W, Kim S-H, Kim K-W. Hypoxia-inducible factor (HIF-1) α: its protein stability and biological functions. Exp Mol Med. 2004;36(1):1–12.
37. Koivunen P, Hirsila M, Gunzler V, Kivirikko KI, Myllyharju J. Catalytic properties of the asparaginyl hydroxylase (FIH) in the oxygen sensing pathway are distinct from those of its prolyl 4-hydroxylases. J Biol Chem. 2004;279(11):9899–904.
38. Loenarz C, Schofield CJ. Expanding chemical biology of 2-oxoglutarate oxygenases. Nature chemical biology. 2008;4(3):152–6.
39. Iommarini L, Porcelli AM, Gasparre G, Kurelac I. Non-Canonical Mechanisms Regulating Hypoxia-Inducible Factor 1 Alpha in Cancer. Front Oncol. 2017;7:286.
40. MacKenzie ED, Selak MA, Tennant DA, Payne LJ, Crosby S, Frederiksen CM, et al. Cell-permeating alpha-ketoglutarate derivatives alleviate pseudohypoxia in succinate dehydrogenase-deficient cells. Mol Cell Biol. 2007;27(9):3282–9.
41. Wheaton WW, Chandel NS. Hypoxia. 2. Hypoxia regulates cellular metabolism. Am J Physiol Cell Physiol. 2011;300(3):C385-93.
42. Fuhrmann DC, Brune B. Mitochondrial composition and function under the control of hypoxia. Redox Biol. 2017;12:208–15.
43. Solaini G, Baracca A, Lenaz G, Sgarbi G. Hypoxia and mitochondrial oxidative metabolism. Biochim Biophys Acta. 2010;1797(6–7):1171–7.
44. Alberti K. The biochemical consequences of hypoxia. J Clin Pathol. 1977;3(1):14–20.
45. Garofalo O, Cox D, Bachelard H. Brain levels of NADH and NAD + under hypoxic and hypoglycaemic conditions in vitro. Journal of neurochemistry. 1988;51(1):172–6.
46. Muz B, de la Puente P, Azab F, Azab AK. The role of hypoxia in cancer progression, angiogenesis, metastasis, and resistance to therapy. Hypoxia (Auckl). 2015;3:83–92.

Figures

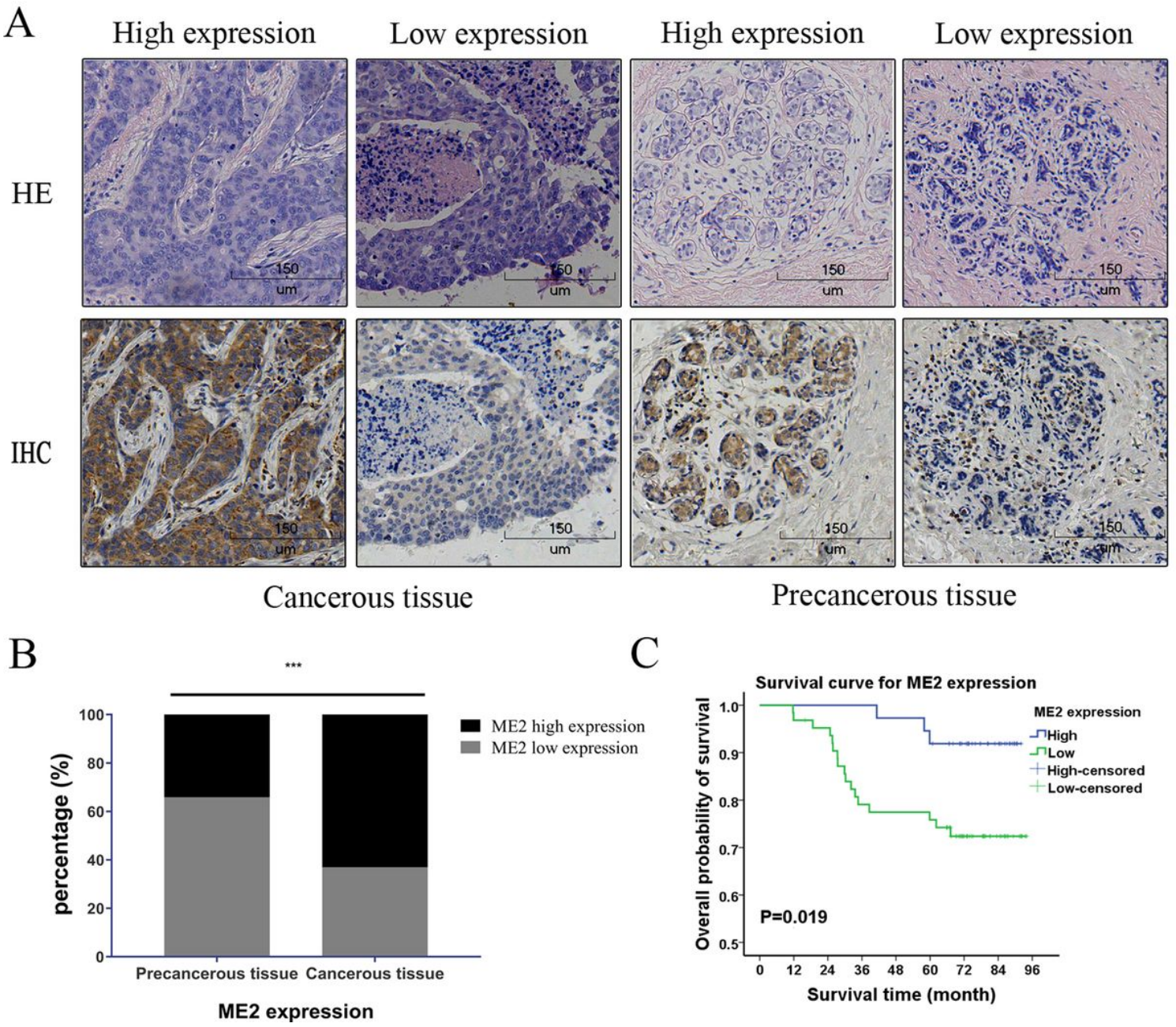

Figure 1

The expression of ME2 in breast cancer and precancerous tissue and its association with overall survival (OS). One hundred female breast cancer patients were retrospectively retrieved and analyzed in this study as described in Materials and Methods. (A) Representative hematoxylin staining and IHC analysis of ME2 in human breast cancerous and precancerous specimens. The scale bar is 150 μm. (B) The high expression of ME2 was displayed in cancerous tissue compared to the matched precancerous tissue. (C) Patients with high expression of ME2 in breast cancerous tissue had a worse OS than those with low expression. Survival analyzed by Kaplan–Meier method. *** P < 0.001.

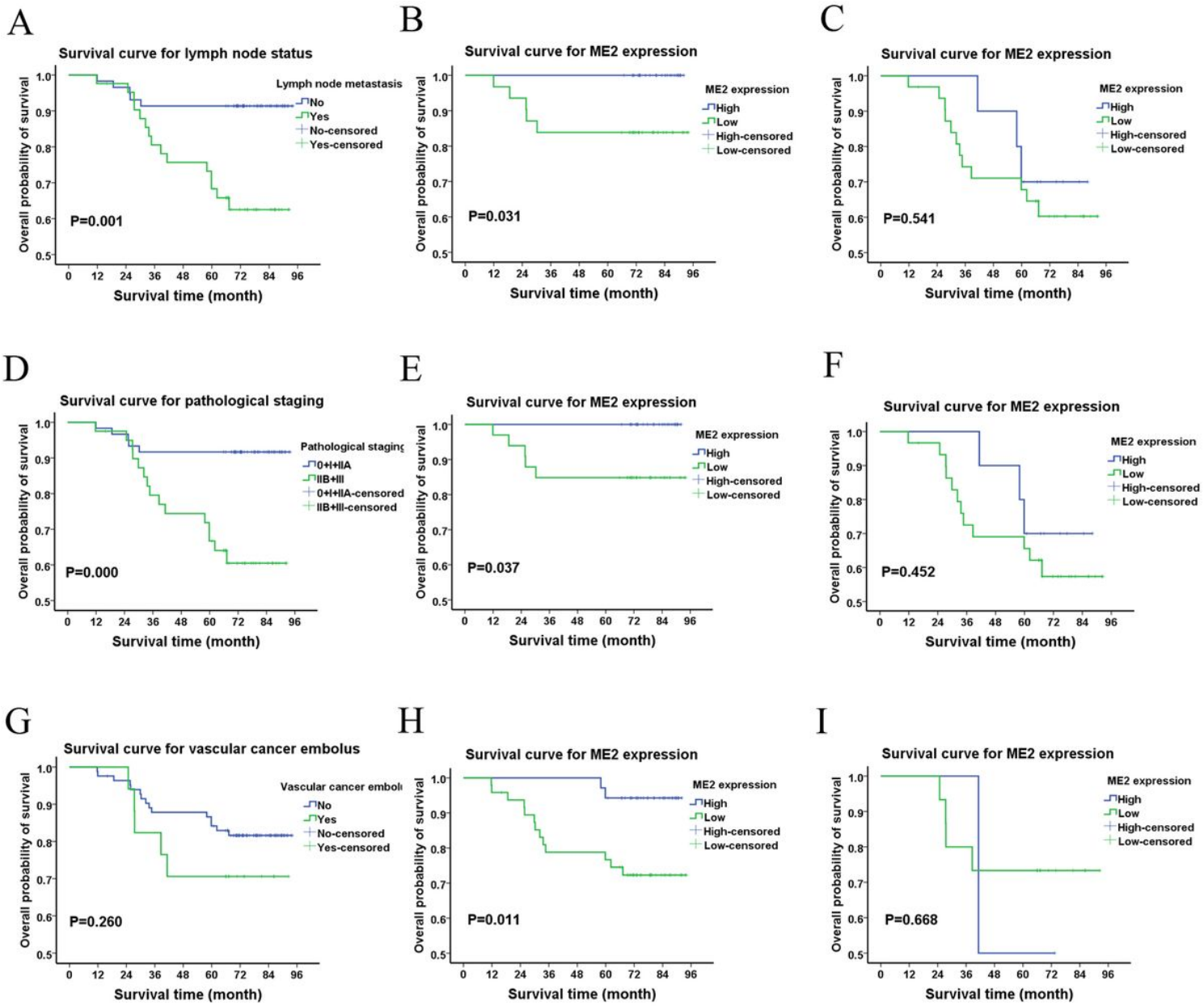

Figure 2

ME2 is associated with metastasis-related indicators. (A) Lymph node metastasis status put a clear association with poor prognosis (χ2=10.691, P=0.001). (B) In the subgroup of patients with no lymph node metastasis, ME2 high expression was worse factors with prognosis (χ2=4.664, P=0.031). (C) In the subgroup of patients with lymph node metastasis, ME2 expression has no significant effect on OS (χ2=0.374, P=0.541). (D) Pathological staging was divided into earlier staging (0-IIA) and advanced staging (IIB-III). The advanced staging was worse indicator for survival compare to earlier staging (χ2=12.711, P=0.000). (E) In the subgroup of earlier staging, ME2 high expression was associated with poor prognosis (χ2=4.362, P=0.037). (F) In the subgroup of advanced staging, ME2 expression has no significant effect on OS (χ2=0.565, P=0.452). (G) There was no significant survival difference of patients with or without vascular cancer embolus (χ2=1.268, P=0.260). (H) In the subgroup of patients without vascular cancer embolus, ME2 high expression was associated with poor prognosis (χ2=6.473, P=0.011).

(I) In the subgroup of patients with vascular cancer embolus, ME2 expression has no significant effect on OS ($\chi 2=0.184$, $P=0.668$). Survival analyzed by Kaplan–Meier method.

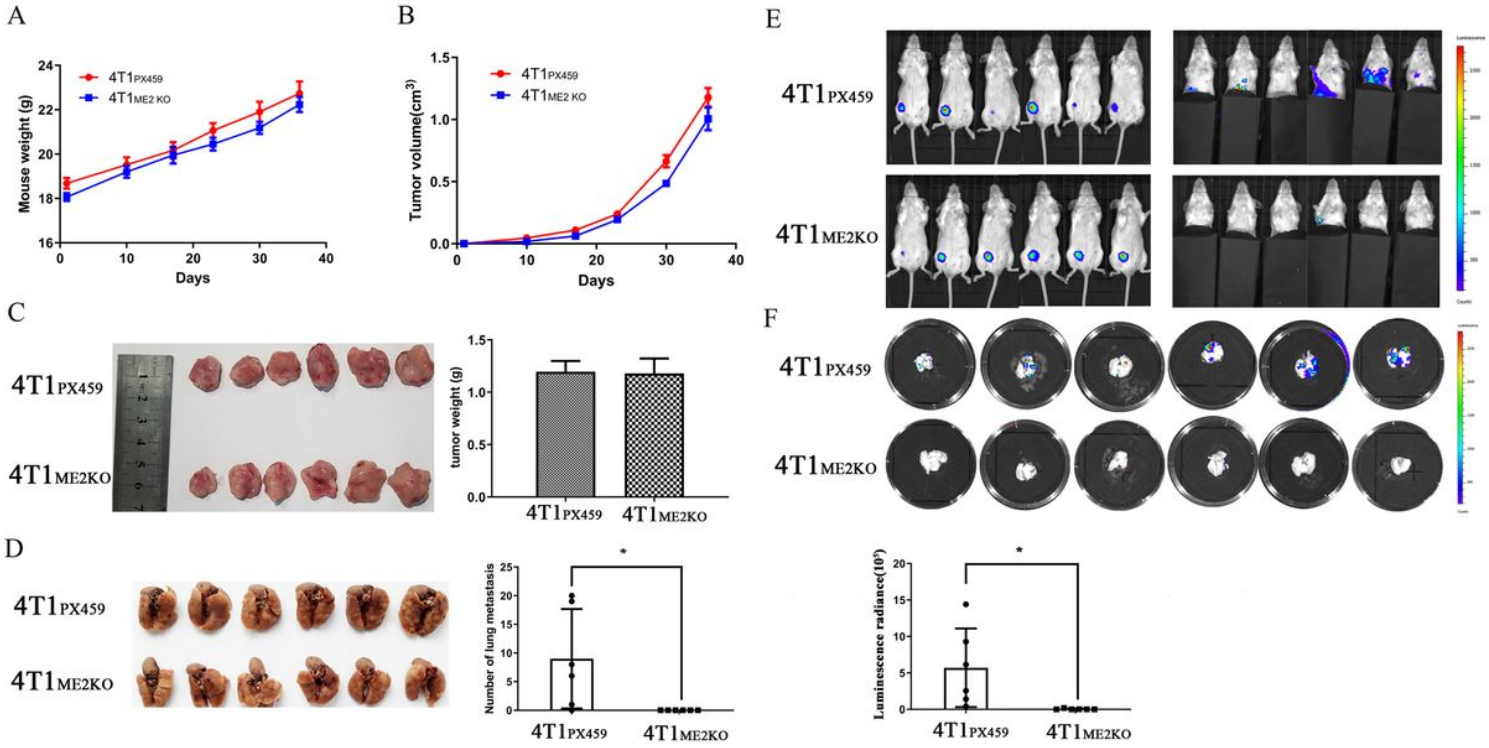

Figure 3

ME2 knockout significantly inhibits breast cancer lung metastasis in vivo. Six-week-old female BALB/c mice were orthotopically inoculated with 1×105 4T1 cells, sacrificed after 5 weeks, record tumor weight and scored the lung metastasis as described in Materials and Methods. (A & B) Body weight and tumor growth curve of BALB/c mice inoculated with 4T1ME2KO and control 4T1PX459. (C) The tumor size and weight. (D) The lung metastatic nodules. (E) Bioluminescence intensity of the tumors formed by 4T1ME2KO and control 4T1PX459. Left panels, the primary tumor. Because the bioluminescence intensity of the primary tumors was too strong, the bioluminescence of the lung metastasis was not revealed. Right panels, the bioluminescence emitted by lung metastasis was revealed after primary tumor bioluminescence was covered up. (F) Bioluminescence imaging of the lungs from mice inoculated with 4T1ME2KO or 4T1PX459. N= 6 per group. Data are mean ± SD from a single experiment. * $P < 0.05$. Data of (A-D) and (E-F) are from 2 independent experiments.

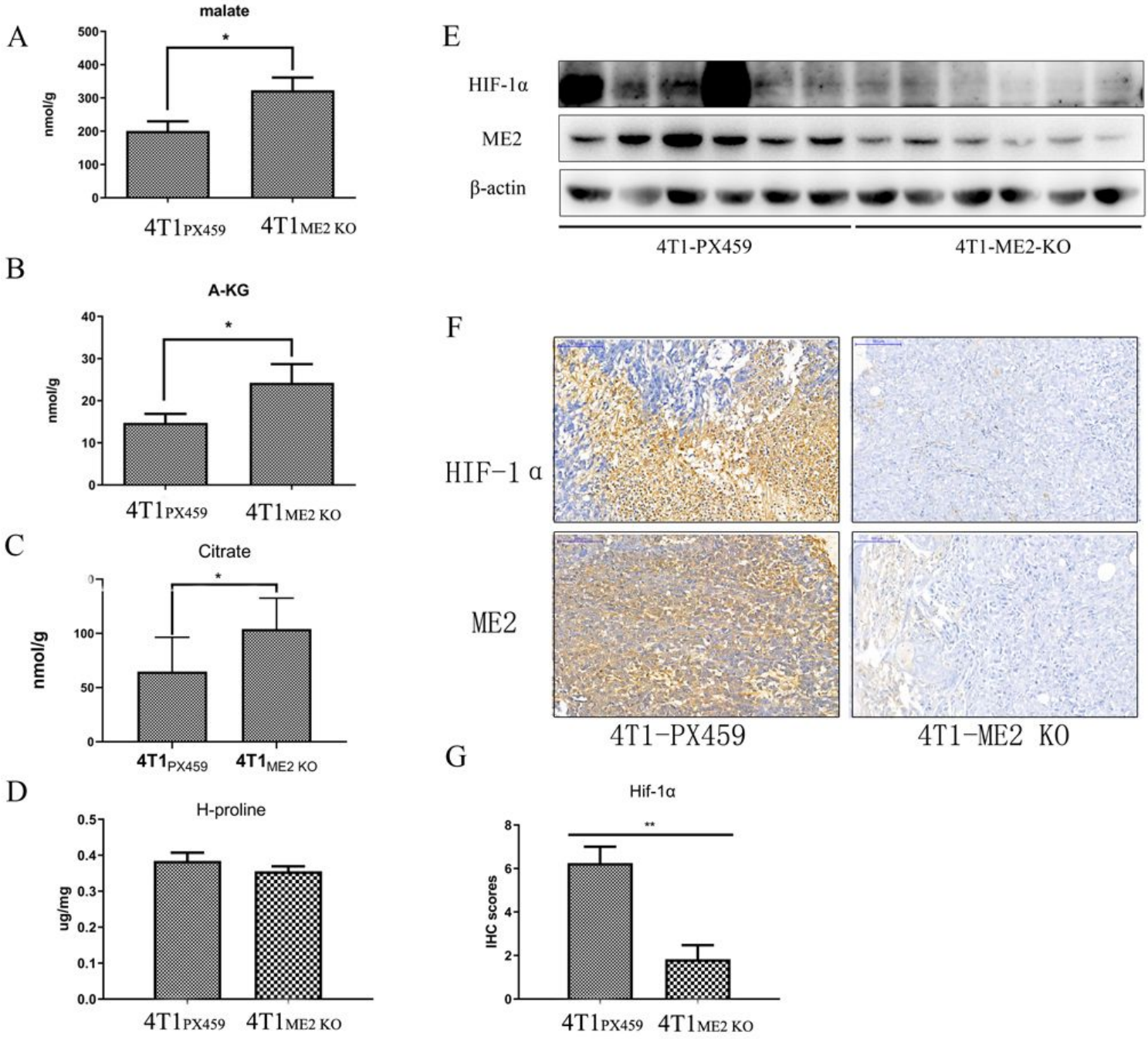

Figure 4

ME2 knockout reduces HIF-1α level and increases the concentrations of TCAC intermediates in vivo. The metabolite of mouse tumor tissue was extracted for analysis as described in Materials and Methods. (A-C) 4T1ME2KO-derived tumor tissues had a higher level of concentration (nmol/gram wet tissues) of malate, α-KG and citrate than 4T1px459-derived tumors. (D) The level of collagen hydoxyproline (H-proline) was comparable between 2 groups. (E-G) Western blot and IHC of HIF-1α expression in 4T1ME2KO-derived and 4T1PX459-derived tumors. The expression of ME2 in 4T1ME2KO-derived tumors may be due to the interstitial cells. N= 6 per group. Data are mean ± SD from a single experiment. * $P < 0.05$. ** $P < 0.01$.

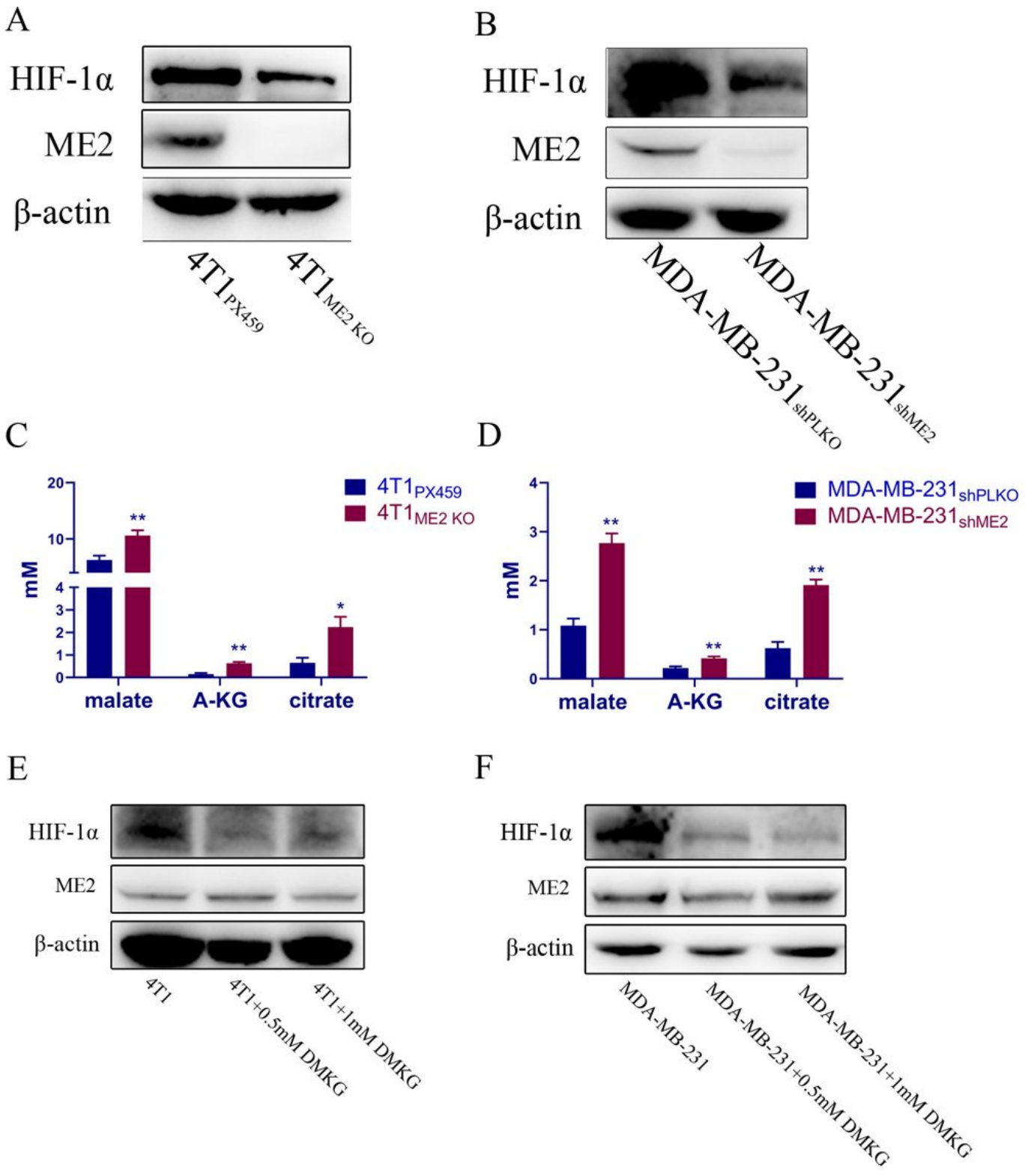

Figure 5

ME2 knockout or knockdown increases the concentrations of TCAC intermediates and decreases HIF-1α level. 4T1 and MDA-MB-231 cells were cultured under 1% oxygen for 4 hours and then collected for analysis as described in Materials and Methods. (A & B) HIF-1α level in ME2 knockout or knockdown cells and control cells. (C & D) The concentrations of TCAC intermediates malate, citrate, and α-KG in ME2

knockout or knockdown cells and control cells. (E & F) HIF-1α in 4T1 and MDA-MB-231 with or without dimethyl α-KG (DMKG) under hypoxia. Data are mean ± SD * P < 0.05, ** P < 0.01.

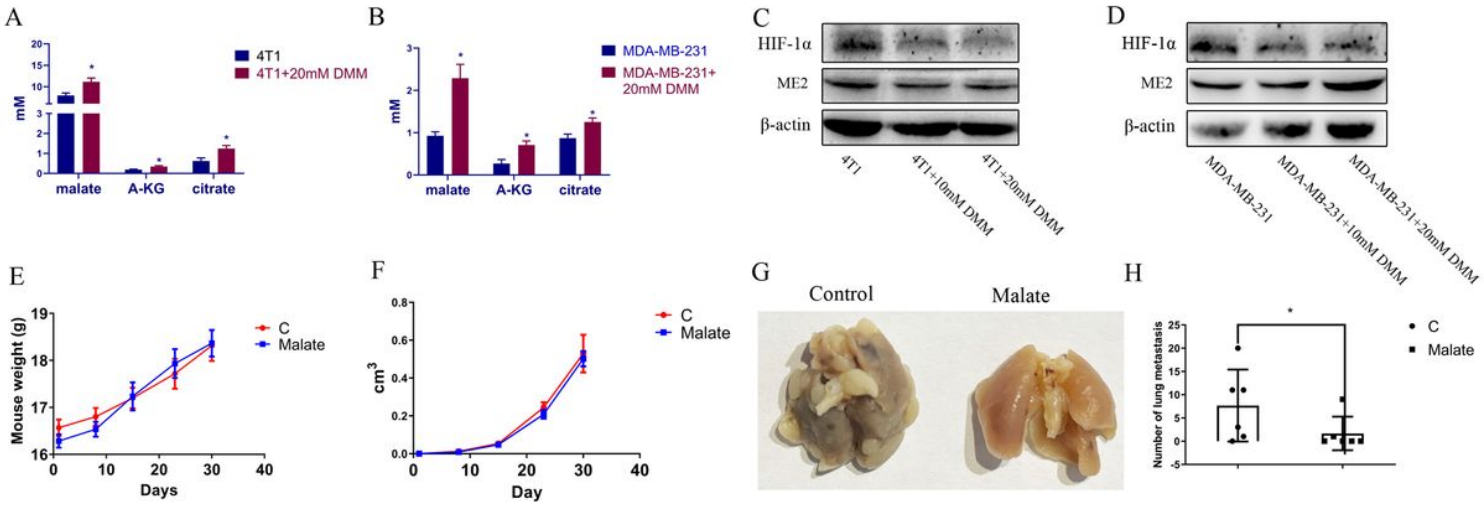

Figure 6

The effect of malate treatment on breast cancer cells. Cells were incubated in medium containing indicated concentrations of dimethyl malate (DMM) and cultured under 1% hypoxia for 4 hours. The cells were collected for analysis as described in Materials and Methods. (A & B) Concentrations of malate, α-KG and citrate in cells with or without DMM under hypoxia. (C & D) HIF-1α in 4T1 and MDA-MB-231 with or without DMM under hypoxia. (E & F) 4T1 cells were implanted orthotopically into mammary fat pads of BALB/c mice. Mice were randomly divided into two groups and injected intraperitoneally with phosphate buffer saline (control) or malate (50 mg/kg, dissolved in PBS) once a day for three weeks. Body weight and tumor growth curve of BALB/c mice treatment with or without malate. (G & H) The lung metastatic nodules. Data are mean ± SD from a single experiment. * P < 0.05, ** P < 0.01.

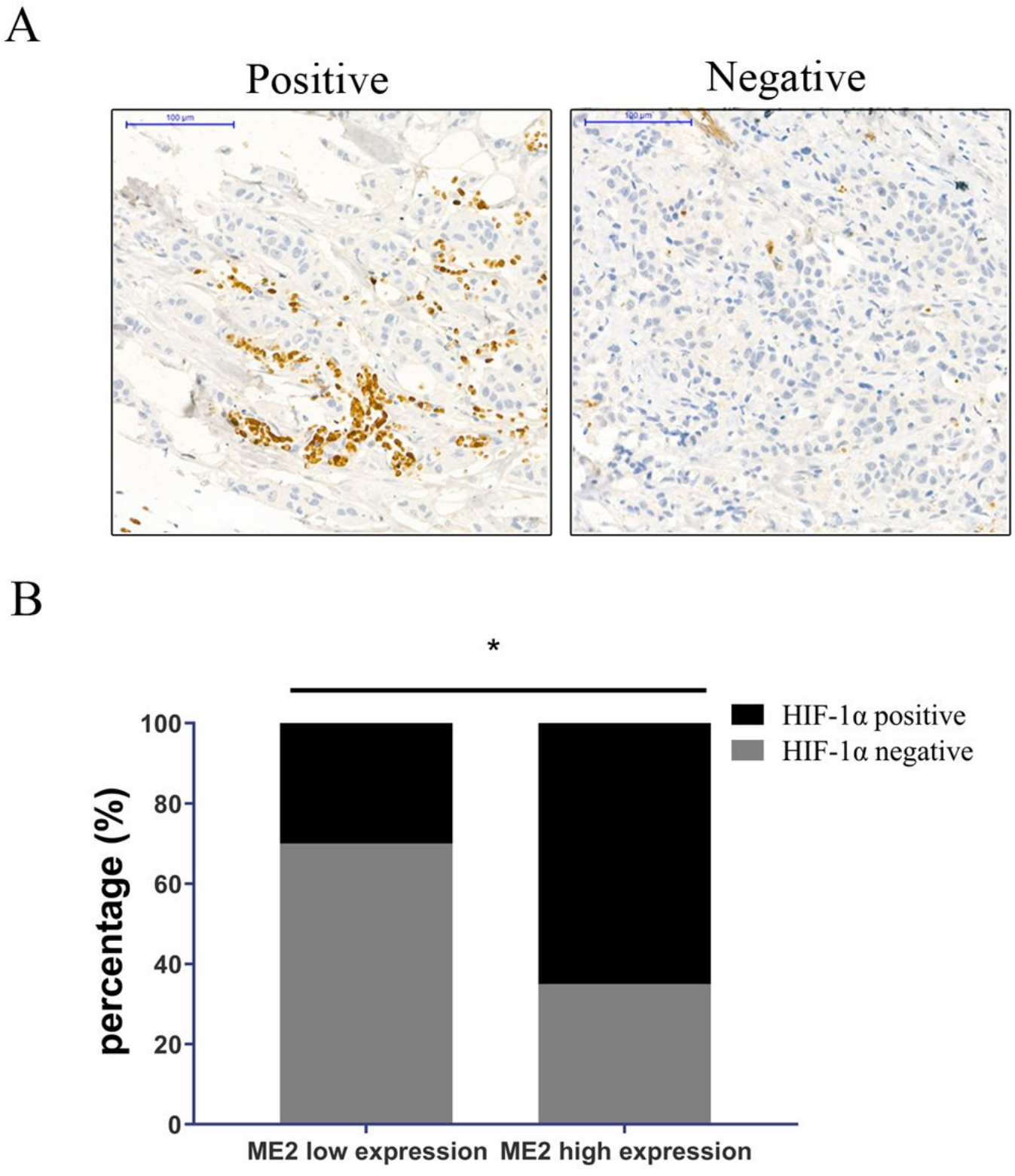

Figure 7

ME2 expression is associated with HIF-1α level in human breast cancer. Randomly selected 20 samples with low expression of ME2 and 20 samples with high expression of ME2 for HIF-1α detect by IHC. (A) Representative IHC analysis of HIF-1α in human breast cancer specimens. The scale bar is 100 μm. (B) Association between HIF-1α and ME2 expression. * $P < 0.05$.

Supplementary Files

This is a list of supplementary files associated with this preprint. Click to download.

- Supplementary201223.docx